

Estimation of Molecular Linear Free Energy Relationship Descriptors. 4. Correlation and Prediction of Cell Permeation

James A. Platts,¹ Michael H. Abraham,^{1,3}
Anne Hersey,² and Darko Butina²

Received February 1, 2000; accepted May 4, 2000

Purpose. The passage of molecules across cell membranes is a crucial step in many physiological processes. We therefore seek physical models of this process, in order to predict permeation for new molecules, and to better understand the important interactions which determine the rate of permeation.

Methods. Several sets of cell permeation data reported by Collander have been correlated against calculated Linear Free Energy Relation (LFER) descriptors. These descriptors, taken as the sum of fragmental contributions, cover the size, polarity, polarizability, and hydrogen bonding capacity of each molecule.

Results. For 36 values of permeation into *Chara ceratophylla* cells, a model (sd = 0.24) dominated by hydrogen bond acidity is found, while for 63 rates of permeation values into *Nitella* cells a very similar model yields sd = 0.46. Comparisons between the two cell types are made directly for 17 compounds in both data sets, indicate differences of a similar magnitude to the standard deviations of the above models. The two data sets can be combined to yield a generic model of rates of permeation into cells, resulting in an sd value of 0.46 for a total of 100 data points.

Conclusions. Models allowing accurate prediction of cell permeation have been constructed using 100 experimental data. We demonstrate that hydrogen bond acidity is the dominating factor in determining cell permeation for two distinct species of algal cell.

KEY WORDS: hydrogen bonding; LFER; permeation; cell walls.

INTRODUCTION

The absorption of molecules into the body or through membranes within the body is of great importance in drug design and pharmacology. Absorption of drugs through the skin can avoid problems with other administration routes (1), allowing for example the direct application of anti-inflammatory drugs (2). Similarly, the ability of drugs to cross cell-wall membranes must be a major factor in their bioavailability and activity (3). Predictive models for such processes are therefore highly desirable, allowing molecular characteristics to be tailored to the absorption process of interest.

By far the most studied of such process is the rate of permeation of compounds from aqueous solution through human skin. Many attempts (4,5) have been made to model this

process using logP(oct), the octanol-water partition coefficient, either on its own or in conjunction with other parameters such as molecular weight or volume. The importance of hydrogen bonding in skin permeation has been stressed by Abraham (6) and Raevsky (7), both of whom have reported models wherein hydrogen bond acidity or basicity feature strongly.

Permeation through biological media other than human skin, such as membranes or cell walls, has also been studied, if not to the same extent. In a very early study (8) Collander reported rates of permeation of around 40 non-electrolytes into the giant algal cells *Chara ceratophylla*, and found approximate linear correlations with water-solvent partition coefficients. Some years later, the same author investigated the permeation into algal *Nitella* cells (9) for a rather larger set of non-electrolytes, again finding reasonable linear correlations with solvent partition coefficients. In this study, he argued that the physical characteristics of these cells, especially their size and shape, made them more suitable for such experiments.

In both cases, the authors used water/ether and water/olive oil partitions as model systems, but found that the non-electrolytes fell into various families or sets. This is to be expected if the systems are not very good models. As Collander pointed out, such family behaviour is often observed in comparisons of various water/solvent partitions; as the solvents differ more and more, so does family behaviour become more pronounced (10). The *Chara ceratophylla* data set was recently re-visited by Raevsky and Schaper (7), who found a strong dependence of permeation on the hydrogen bond capacity of the non-electrolytes. However, these authors chose to analyse only 27 of the available 37 data points, omitting the remainder with no comment.

Scales of hydrogen bond acidity and basicity form a major part of the Linear Free Energy Relation (LFER) method of Abraham and co-workers (11,12). This method treats solvation effects as a linear combination of free-energy related descriptors, according to the general Eq. (1)

$$\log SP = c + r \cdot R_2 + s \cdot \pi_2^H + a \cdot \sum \alpha_2^H + b \cdot \sum \beta_2^H + v \cdot V_x \quad (1)$$

where R_2 is an excess molar refraction, essentially describing dispersion effects, π_2^H is a joint polarity/polarizability term, $\sum \alpha_2^H$ and $\sum \beta_2^H$ are the hydrogen bond acidity and basicity, respectively, and V_x is McGowan's characteristic volume (13).

A wide range of physicochemical and biological processes have been analysed in this manner, including water-solvent and gas-solvent partition coefficients, chromatographic retention data and related properties, characterisation of chemical sensors, membrane irritation and pungency thresholds, blood-brain distribution, brain perfusion, and skin permeation: see ref. (12) for a recent review. In this manner, not only are useful predictive models developed but also the nature of the phases involved can be elucidated. For example, for 51 human skin permeation values (logKp), the following model was reported:

$$\log Kp (\text{cm s}^{-1}) = -5.13 + 0.44 R_2 - 0.49 \pi_2^H - 1.48 \sum \alpha_2^H - 3.44 \sum \beta_2^H + 1.94 V_x \quad (2)$$

$$n = 51, \quad R^2 = 0.958, \quad R_{CV}^2 = \dots,$$

$$sd = 0.213, \quad F = 213$$

¹ Department of Chemistry, University College London, 20 Gordon St., London WC1H 0AJ, U.K.

² BioMet Technology & Informatics Group, Glaxo Wellcome Research and Development, Park Road, Ware SG12 0DP, U.K.

³ To whom correspondence should be addressed. (e-mail: m.h.abraham@ucl.ac.uk)

Here, and throughout this paper, n is the number of data points in the regression, R^2 is the square of the overall correlation coefficient, R_{CV}^2 the 'leave-one-out' cross-validated R^2 , a measure of the internal self-consistency of the model (R_{CV}^2 was not quoted by these authors), sd the standard deviation, and F Fischer's F ratio.

As $\log K_p$ relates to permeation from aqueous solution through skin, the coefficients in Eq. (2) relate to the difference between skin and water, rather than to skin directly. Equation (2) clearly shows hydrogen bonding to dominate skin permeation, acting to reduce $\log K_p$, i.e., keeping the compound in the aqueous phase. Molecular volume increases the rate of permeation, which can be ascribed to favourable dispersion interactions in the stratum corneum, and to the removal of unfavourable cavity effects in the aqueous phase.

We have recently developed an automated method for the calculation from structure of the descriptors used in Eq. (1) (14). This method estimates molecular descriptors as the sum of fragment values found from linear regression, employing 81 fragments for R_2 , π_2^H , and $\Sigma\beta_2^H$, and a separate 46 fragment scheme for $\Sigma\alpha_2^H$. V_x is exactly calculable for any structure. With this approach, we were able to predict descriptors, which cover a range of around 5 log units, with an accuracy of around 0.10–0.15 log units. We have subsequently demonstrated that this approach is capable of predicting water-octanol, chloroform, and -cyclohexane partition coefficients of large, complex drug-like molecules with an accuracy of between 0.70 and 1.0 log units (15), similar to many commercially available packages.

In the current study, we have applied the same methodology to Collander's permeation data, i.e., for both *Chara ceratophylla* and *Nitella* algal cells. The purpose of this is two-fold: (i) to develop a model of the form of Eq. (1) for each data set; (ii) to compare permeation into each cell type, searching for similarities and differences in the models. In doing this, we hope to establish a general model for the permeation of any non-electrolytic organic compound into such cells.

METHODOLOGY

Descriptors for molecules were calculated as described in ref. (14). Molecular structures were input as Daylight SMILES codes, and the relevant fragment contributions identified. These calculations were performed on a Silicon Graphics O². Having calculated descriptors for each molecule in each set, separate LFER equations were developed using multiple linear regression (MLR). All such regressions were performed using the JMP package, published by SAS software, and employed the standard t -test in order to check significance at the 95% level. Following this, the two data sets were combined and same MLR process repeated for the entire set.

RESULTS AND DISCUSSION

In a seminal early study (8), Collander reported rates of permeation of 45 non-electrolytes from aqueous solution through cells of *Chara ceratophylla*. However, eight of these data were reported as $<3 \times 10^9 \text{ cm s}^{-1}$, and could not be modelled with the rest of the data. Collander found approximate linear relations between the remaining data and water-ether and water-olive oil partition data, indicating qualitatively the

molecular properties responsible for permeation. Recently, Raevsky and Schaper (7) revisited this data set, finding a linear correlation between permeation values and hydrogen bond donor strength.

With 37 data points and considerable chemical diversity in this set, we were able to construct an equation of the form of Eq. (1) for rates of permeation through *Chara ceratophylla* cells, which we will denote $\log k_{CC}$, shown here as Eq. (3)

$$\begin{aligned} \log k_{CC} (\text{cm s}^{-1}) = & -2.213 - 1.030 \pi_2^H - 3.016 \Sigma\alpha_2^H \\ & - 1.335 \Sigma\beta_2^H + 0.710 V_x \end{aligned} \quad (3)$$

$n = 36, \quad R^2 = 0.962, \quad R_{CV}^2 = 0.935,$
 $sd = 0.245, \quad F = 195$

Observed and calculated $\log k_{CC}$ values for all 37 molecules are reported in Table I. One compound, lactamide, was omitted from the regression as a strong outlier, and one relatively large ($R^2 = 0.53$) correlation was found for π_2^H vs. $\Sigma\alpha_2^H$. The dominating term in Eq. (3) is the hydrogen bond acidity, $\Sigma\alpha_2^H$,

Table I. Observed and Calculated $\log k_{CC}$ Values on Eq. (3)

Name	$\log k_{CC}$	
	obs	calc
Methanol	0.00	-0.10
Ethanol	-0.25	0.00
Urethane	-0.37	-0.24
Methylurethane	-0.40	-0.34
Triethylcitrate	-0.43	-0.53
Trimethylcitrate	-0.62	-0.83
Antipyrine	-0.66	-0.25
Cyanamide	-0.68	-0.45
i-Valeramide	-0.72	-0.84
Butyramide	-0.77	-0.95
Propionamide	-0.89	-1.05
Monochlorohydrin	-1.05	-1.59
Propyleneglycol	-1.06	-1.32
Diacetin	-1.10	-0.94
Glycerinmonoethylether	-1.11	-1.24
Formamide	-1.11	-1.29
Succinimide	-1.23	-1.19
Diethylurea	-1.23	-1.37
Acetamide	-1.28	-1.15
Glycerine monomethylether	-1.37	-1.34
Ethyleneglycol	-1.37	-1.43
Dimethylurea	-1.47	-1.57
Monacetin	-1.80	-1.75
Ethylurea	-1.92	-1.73
Thiourea	-2.11	-2.32
Methylurea	-2.17	-1.83
Lactamide	-2.25	-1.21
Diethylmalonamide	-2.37	-2.44
Urea	-2.40	-2.07
Methenamine	-2.59	-2.76
Dicyanodiamide	-2.96	-3.03
Methoxyurea	-3.08	-3.55
Glycerin	-3.13	-2.78
Mucic acid diethylester	-3.28	-3.16
Malonamide	-3.85	-3.97
Erythritol	-4.34	-4.12
Arabinose	-4.51	-4.11

which lowers the rate of permeation of a compound. Of lesser importance are the hydrogen bond basicity, $\Sigma\beta_2^H$, and the solute polarity/polarisability, π_2^H , both of which also lower the rate of permeation, whilst molecular size, as V_x , increases the rate. The $r \cdot R_2$ term was not statistically significant and has been omitted in Eq. (3).

The coefficients of Eq. (3) are not simply fitting constants, but describe the differences between the cell environment and aqueous solution, from which the molecules permeate into the cell. Thus, the very large coefficient of $\Sigma\alpha_2^H$ indicates that the cell interior is very much less basic than bulk water, a much bigger difference than between human skin and water. The negative coefficients of π_2^H and $\Sigma\beta_2^H$ show that the cell is both less polar and less acidic than water, though these differences are not as marked as with $\Sigma\alpha_2^H$. Indeed, a $\Sigma\beta_2^H$ coefficient of -1.335 is very small when compared to many known systems: for example, the $\Sigma\beta_2^H$ coefficient for octanol-water partition is -3.460 and for chloroform-water it is -3.467 (15). Thus, the cell is not as acidic as bulk water, but is considerably more so than either octanol or chloroform. Finally, the positive V_x coefficient could be ascribed to unfavourable cavity effects in the aqueous phase, or to dispersion attractions in the cell.

Equation (3) represents a general model for the permeation of organic compounds into *Chara ceratophylla* cells, and as such can be used to predict new values of $\log k_{CC}$. However, this model is only valid within the descriptor ranges used for training the model—these are shown in Table II. In general, the upper limits are rather high—for example in our recent study (15) of 140 drugs and environmental chemicals, only four tri-peptides had $\Sigma\beta_2^H$ greater than 2.69. However, the lower limits of the descriptor ranges, most notably π_2^H and $\Sigma\beta_2^H$, suggest that very non-polar molecules may not be modelled especially well by Eq. (3).

The above model is in agreement with Raevsky and Schaper's finding, summarised as Eq. (4) below, that $\log k_{CC}$, which they denoted $\log[\text{Per}]$, is closely related to hydrogen bond donor strength for a subset of the total data-set discussed above.

$$\log[\text{Per}] = 0.83 + 0.59 \Sigma C_d \quad n = 27, \quad R^2 = 0.815, \quad (4)$$

$$R_{CV}^2 = 0.783, \quad sd = 0.49$$

The difference in sign between coefficients is consistent, since Raevsky (7) defines hydrogen bond donors to have negative ΣC_d values, both models indicating that the rate of permeation decreases with increasing H-bond donor strength. However, the authors reported no dependence of $\log[\text{Per}]$ with either polarisability or size (as MW), quite unlike Eq. (3) which has terms for both properties. The much-improved statistics of Eq. (3)—the standard deviation is less than half that of Eq. (4)—and the larger data set used indicate these factors do indeed have an effect on the rate of permeation.

Collander (9) reported a second set of permeation data in 1954, this time on the rate of permeation of *Nitella* cells to

more than 60 non-electrolytes. Again, linear models with ether-water and olive-oil water partitions were developed with some success. We have applied the same methodology used to develop Eq. (3) to this data, resulting in Eq. (5):

$$\log k_{Nit} \text{ (cm s}^{-1}\text{)} = -1.969 + 0.516 R_2$$

$$- 1.267 \pi_2^H - 3.409 \Sigma\alpha_2^H$$

$$- 2.094 \Sigma\beta_2^H + 0.980 V_x \quad (5)$$

$$n = 63, \quad R^2 = 0.881,$$

$$R_{CV}^2 = 0.825, \quad sd = 0.462, \quad F = 84$$

Observed and calculated values of $\log k_{Nit}$ are reported in Table III. One large cross-correlation, $R^2 = 0.59$, was found for π_2^H vs. $\Sigma\beta_2^H$. Descriptor ranges used to determine Eq. 5 are reported in Table IV.

Equation (5) represents, to our knowledge, the first such attempt to model this data set since publication. The fit statistics are not as impressive as for Eq. (3), probably as a result of the wider range of compounds, and the greater range of values $\log k$ takes in this set. However, the accuracy is sufficient to observe the factors determining the rate of permeation into *Nitella* cells, and they are remarkably similar to those for *Chara ceratophylla*. Hydrogen bond acidity is again dominant, with basicity and polarity making smaller negative contributions, and volume increasing the rate of permeation. R_2 is now significant at the 95% level, but makes only a small positive contribution to $\log k_{Nit}$. On this basis it appears that *Nitella* and *Chara ceratophylla* cells are very similar environments, a possibility discussed further below.

In addition to the permeation of compounds into living *Nitella* cells, as with the *Chara ceratophylla* cells discussed above, Collander also reported permeation data into dead cells. It was suggested that this partition process is dependent on molecular weight, and not on other physicochemical properties such as lipophilicity. Applying our LFER approach to this data, we find an excellent correlation with only one descriptor, Eq. (6)

$$\log k_{Nit}^{\text{Dead}} = -3.103 - 0.319 V_x \quad n = 64,$$

$$R^2 = 0.934, \quad R_{CV}^2 = 0.927, \quad (6)$$

$$sd = 0.035, \quad F = 876$$

The difference between living and dead *Nitella* cells is striking—rates of permeation into dead cells show no dependence on polarity or hydrogen bonding, but depend solely on molecular volume. In addition, the coefficient of V_x is rather small—less than one-third of that found for the living cells, indicating that the dead cell is a relatively easy barrier to cross. The negative coefficient of V_x means that smaller molecules cross the (dead) cell wall more easily than large ones, unlike equations 3 & 5. This suggests a fundamental difference in the way molecules cross living and dead cell walls, i.e., $\log k^{\text{Dead}}$ is a purely diffusion-controlled process with no specific chemical interactions between molecule and cell.

Collander considered partition into the living protoplasm, rather than the mixture of living and dead tissue that constitutes an actual cell, to be the interesting and important factor at play. These processes are linked through Eq. (7)

$$1/k_{\text{proto}} = 1/k_{\text{live}} - 1/k_{\text{dead}} \quad (7)$$

Table II. Descriptor Ranges Used in Eq. (3)

	R_2	π_2^H	$\Sigma\alpha_2^H$	$\Sigma\beta_2^H$	V_x
Min	0.31	0.45	0.00	0.39	0.3082
Max	1.53	1.92	1.12	2.69	2.0813

Table III. Observed and Calculated $\log k_{\text{Nit}}$ Values on Eq. (8)

Name	$\log k_{\text{Nit}}$	
	obs	Calc
Ethyl acetate	-2.75	-3.38
Methyl acetate	-2.89	-3.38
sec-Butanol	-3.67	-3.49
Methanol	-4.09	-3.49
n-Propanol	-3.81	-3.5
Ethanol	-3.95	-3.52
Paraldehyde	-4.05	-3.57
Urethane	-4.21	-3.63
i-Propanol	-3.81	-3.64
Acetonylacetone	-3.73	-3.64
Diethyleneglycol monobutylether	-3.97	-3.85
Dimethylcyanamide	-4.09	-3.86
t-Butanol	-3.71	-3.86
Glycerol diethylether	-3.67	-3.88
Ethoxyethanol	-3.88	-3.89
Methyl carbamate	-4.34	-3.91
Triethyl citrate	-4.89	-3.97
Methoxyethanol	-4.02	-4.09
Triacetin	-4.4	-4.12
Dimethylformamide	-4.14	-4.21
Triethyleneglycol diacetate	-4.34	-4.29
Pyramidone	-4.35	-4.29
Diethyleneglycol monoethylether	-4.24	-4.44
Caffeine	-5.00	-4.50
Cyanamide	-4.61	-4.55
Tetraethyleneglycol dimethylether	-3.84	-4.59
Pinacol	-5.19	-4.66
Diacetin	-5.19	-4.71
Methylpentanediol	-5.47	-4.74
Antipyrone	-3.93	-4.74
i-Valeramide	-4.93	-4.76
1,6-Hexanediol	-5.45	-4.77
n-Butyramide	-5.07	-4.87
Diethyleneglycol monomethylether	-4.38	-4.89
Trimethyl citrate	-5.30	-4.94
Propionamide	-5.21	-5.11
Formamide	-5.54	-5.12
Acetamide	-5.35	-5.18
Succinimide	-5.29	-5.28
Glycerol monoethylether	-5.51	-5.40
N,N-Diethylurea	-4.92	-5.42
1,5-Pentanediol	-5.59	-5.47
Dipropylenglycol	-5.29	-5.51
Glycerol monochlorohydrin	-5.78	-5.52
1,3-Butanediol	-5.73	-5.62
2,3-Butanediol	-5.41	-5.68
1,2-Propanediol	-5.55	-5.77
N,N-Dimethylurea	-5.20	-5.82
1,4-Butanediol	-5.73	-5.85
Ethylene glycol	-5.69	-5.92
Glycerol monomethylether	-5.65	-5.92
N,N'-Dimethylurea	-5.93	-5.92
1,3-Propanediol	-5.86	-6.00
Thiourea	-6.63	-6.44
Diethyleneglycol	-5.56	-6.42
Methylurea	-6.17	-6.49
Urea	-6.4	-6.89
Triethyleneglycol	-5.91	-7.00
Tetraethyleneglycol	-6.25	-7.15
Dicyandiamide	-6.57	-7.34

Table III. Continued

Name	$\log k_{\text{Nit}}$	
	obs	Calc
Hexanetriol	-7.55	-7.38
Hexamethylenetriamine	-7.95	-7.41
Pentaerythritol	-9.77	-9.70

Since $\log k_{\text{dead}}$ is dependent solely on molecular size, $\log k_{\text{proto}}$ is expected to show very similar dependence on polarity and hydrogen bonding as $\log k_{\text{live}}$. Further, partition into dead cells is generally much faster than partition into living cells, so that $1/k_{\text{dead}}$ is small, and $1/k_{\text{proto}}$ is mostly very close to $1/k_{\text{live}}$. That this is indeed the case is demonstrated by Eq. (8), wherein $\log k_{\text{proto}}$ is correlated in the same manner as used for Eq. (5)

$$\log k_{\text{proto}} = -1.497 + 0.545 R_2 - 1.444 \pi_2^{\text{H}} - 3.823 \Sigma \alpha_2^{\text{H}} - 2.304 \Sigma \beta_2^{\text{H}} + 1.082 V_x \quad (8)$$

$$n = 63, \quad R^2 = 0.875,$$

$$R_{\text{CV}}^2 = 0.779, \quad \text{sd} = 0.517, \quad F = 77$$

Comparing Eqs. (5) and (8), the similarities are obvious. The rate of permeation into both living *Nitella* cells and their protoplasm is dominated by hydrogen bond acidity, with smaller contributions from polarity/polarizability and hydrogen bond basicity.

There are rates of permeation for 27 compounds for both types of cell measured by Collander: these are listed in Table V with their respective $\log k_{\text{CC}}$ and $\log k_{\text{Nit}}$ values. In general the values are similar, the differences varying from 0.01 to 0.55, with a standard deviation of 0.44 log units. Thus, the size of these differences is of the order of the errors in Eqs. (3) and (5), and the two sets of data can be combined: modelling this combined data set (now including lactamide) results in a generic permeation model, Eq. (9)

$$\log k_{\text{gen}} = -2.235 - 0.867 \pi_2^{\text{H}} - 3.143 \Sigma \alpha_2^{\text{H}} - 1.664 \Sigma \beta_2^{\text{H}} + 0.731 V_x \quad n = 100, \quad (9)$$

$$R^2 = 0.886, \quad R_{\text{CV}}^2 = 0.870,$$

$$\text{sd} = 0.437, \quad F = 183$$

A plot of observed vs. calculated $\log k_{\text{gen}}$ values from Eq. (9) is shown in Fig. 1. As before, one large correlation is found between π_2^{H} and $\Sigma \beta_2^{\text{H}}$, with $R^2 = 0.58$. The parallels between the three models of cell permeation are striking - in all cases rates of cell permeation are strongly retarded by solute hydrogen bond acidity, and rather less so by polarity/polarizability and

Table IV. Descriptor Ranges Used in Eq. (8)

	R_2	π_2^{H}	$\Sigma \alpha_2^{\text{H}}$	$\Sigma \beta_2^{\text{H}}$	V_x
Min	0.00	0.37	0.00	0.35	0.1673
Max	1.94	1.81	1.38	2.69	2.0813

Table V. Comparison of Permeation Through *Chara cheratophylla* and *Nitella* Cells

Name	logk _{CC}	logk _{Nit}
Methanol	-4.004	-3.49
Cyanamide	-4.678	-4.55
Formamide	-5.114	-5.12
Ethanol	-4.252	-3.52
Urea	-6.398	-6.89
Acetamide	-5.276	-5.18
Ethyleneglycol	-5.367	-5.92
Methylurethane	-4.398	-3.91
Thiourea	-6.114	-6.44
Methylurea	-6.167	-6.49
Propionamide	-4.886	-5.11
Propyleneglycol	-5.060	-5.77
Dicyanodiamide	-6.959	-7.34
Succinimide	-5.229	-5.28
Urethane	-4.367	-3.63
Dimethylurea	-5.469	-5.92
Monochlorohydrin	-5.046	-5.52
Butyramide	-4.770	-4.87
Glycerinmonomethylether	-5.367	-5.92
i-Valeramide	-4.721	-4.76
Glycerinmonoethylether	-5.114	-5.40
Methenamine	-6.585	-7.41
Diethylurea	-5.229	-5.42
Diacetin	-5.097	-4.71
Antipyrine	-4.658	-4.74
Trimethylcitrate	-4.620	-4.94
Triethylcitrate	-4.432	-3.97

hydrogen bond basicity. Equation (9) seems to open up the possibility that permeation of non-electrolytes into algal cells in general can be predicted by this LFER approach.

A notable feature of Eqs. (3), (5), and (9) is the size of the $\Sigma\alpha_2^H$ term, which is considerably larger than either the π_2^H or $\Sigma\beta_2^H$ terms. This is a rather unusual feature, rarely seen in water-solvent partition equations, and suggests a reason why Collander's correlations with ether-water ($\Sigma\alpha_2^H$ coefficient = -0.097, $\Sigma\beta_2^H$ coefficient = -5.00) and olive oil-water ($\Sigma\alpha_2^H$ coefficient: -1.47, $\Sigma\beta_2^H$ coefficient: -4.92) were only approximate. Two partition or partition-related processes have been put forward in the literature to account mainly for hydrogen bond acidity. $\Delta\log P$ is defined (16) as the difference between a solute's octanol-water and alkane-water logP values, i.e.,

Table VI. Cos θ Values Between Rates of Cell Permeation, Eq. (9), and Model Processes

	cos θ
$-\Delta \log P$	0.92
$\log P_{eh}$	0.73
$\log P(oct)$	0.33
$\log P(cyc)$	0.40

$\Delta\log P = \log P(oct) - \log P(alk)$, and has been suggested as a measure of hydrogen bond acidity (17), although later work (18) suggests that this is an over-simplification (see (18) Eq. (15)). The ethylene glycol - water partition coefficient, as $\log P_{eh}$, has also been suggested as mainly due to solute hydrogen bond acidity but with other factors also being important (19,20). The most detailed LFER equation is given (20) as Eq. (11). The LFER equations for these two systems, Eq. (10) and Eq. (11) allow a direct comparison with the generic cell permeation Eq. (9):

$$\Delta\log P = -0.072 - 0.093 R_2 + 0.528 \pi_2^H + 3.655 \Sigma\alpha_2^H + 1.396 \Sigma\beta_2^H - 0.521 Vx$$

$$n = 288, \quad R^2 = 0.967, \quad sd = 0.173,$$

$$F = 1646 \quad (10)$$

$$\log P_{eh} = 0.336 - 0.075 R_2 - 1.201 \pi_2^H - 3.786 \Sigma\alpha_2^H - 2.201 \Sigma\beta_2^H + 2.085 Vx$$

$$n = 75, \quad R^2 = 0.966, \quad sd = 0.28, \quad F = 386 \quad (11)$$

The opposite signs of coefficients between Eqs. (10) and (11) are purely a result of the definition of $\Delta\log P$. General similarities between the three equations can be seen, most notably the dominance of $\Sigma\alpha_2^H$ in each equation, though small differences are apparent in the coefficients of $\Sigma\beta_2^H$ and Vx . Following Ishihama and Asakawa (21) LFER equations can be thought of as vectors in "descriptor space", and a quantitative measure of equations' similarities is the cosine of the angle between them. In the extreme case of LFER equations being identical, the angle between them, θ , is zero and $\cos \theta = 1.0$. Table VIII presents these $\cos \theta$ values between Eq. (9) and Eqs. (10) and (11), along with values for $\log P(octanol)$ and $\log P(cyclohexane)$ for comparison. These results show that $-\Delta\log P$ ($\cos \theta = 0.92$ or $\theta = 23^\circ$) is the best model of cell permeation. $\log P_{eh}$, with $\theta = 43^\circ$, is only distantly related to permeation, while $\log P(cyc)$ and $\log P(oct)$ ($\theta = 66^\circ$ and 71° , respectively) are not closely related to cell permeation at all.

CONCLUSIONS

We have established that our method of calculating the LFER descriptors R_2 , π_2^H , $\Sigma\alpha_2^H$, $\Sigma\beta_2^H$, and Vx is capable of correlating and predicting permeation processes in two different cell types. Permeability data through *Chara ceratophylla* and *Nitella* cells are found to have remarkably similar dependence on the LFER descriptors, with both equations dominated by hydrogen bond acidity. Dead *Nitella* cells, on the other hand, show no dependence on hydrogen bond capacity or polarity, and are very well modelled by molecular volume alone. We

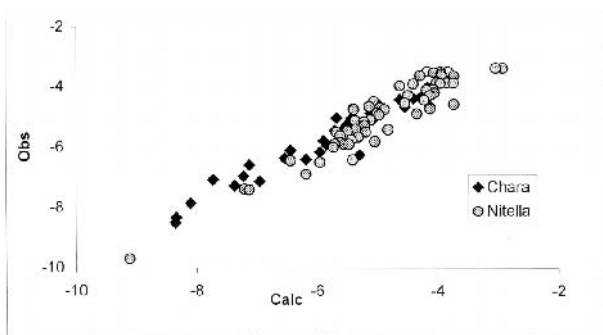


Fig. 1. Plot of observed vs. calculated logk_{gen} values from Eq. (9).

demonstrate that rates of permeation into *Chara ceratophylla* and *Nitella* cells are so similar that the data can be combined to produce a generic model of cell permeation, again dominated by $\Sigma\alpha_2^H$. The similarity between this and $\Delta\log P$, defined as $\log P(\text{oct}) - \log P(\text{alkane})$ is highlighted by the cosine of the angle between the two equations.

ACKNOWLEDGMENTS

JAP is grateful to Glaxo Wellcome for a post-doctoral fellowship.

REFERENCES

1. R. J. Scheuplein and R. L. Bronaugh, *Percutaneous absorption*, in: Goldsmith, L. A. (ed), *Biochemistry and physiology of the skin*, O.U.P., New York, pp. 1255–1295.
2. T. Yano, A. Nakagawa, M. Tsuji, and K. Noda. Skin permeability of various non-steroidal anti-inflammatory drugs in man. *Life Sci.* **39**:1043–1050 (1986).
3. See for example: K. Arimori and M. Nakano. Drug exsorption from blood into the gastro-intestinal tract. *Pharm. Res.* **15**:371–376 (1998).
4. A. Wilschut, W. F. ten Berge, P. J. Robinson, and T. E. McKone. Estimating skin permeation: The validation of five mathematical skin permeation models. *Chemosphere* **30**:1275–1296 (1995).
5. (a) E. J. Lien and H. Gao. QSAR analysis of skin permeability of various drugs in man as compared to *in vivo* and *in vitro* studies in rodents. *Pharm. Res.* **12**:583–587 (1995). (b) R. O. Potts and R. H. Guy. A predictive algorithm for skin permeability—the effects of molecular size and hydrogen bond activity. *Pharm. Res.* **12**:1628–1633 (1995).
6. M. H. Abraham, F. Martins, and R. C. Mitchell. Algorithms for skin permeability using hydrogen bond descriptors: The problem of steroids. *J. Pharm. Pharmacol.* **49**:858–865 (1997).
7. O. A. Raevsky and K.-J. Schaper. Quantitative estimation of hydrogen bond contribution to permeability and absorption processes of some chemicals and drugs. *Eur. J. Med. Chem.* **33**:799–807 (1998).
8. R. Collander and H. Bärlund. Permeabilitätsstudien an *chara ceratophylla*. *Acta Bot. Fenn.* **11**:1–112 (1933).
9. R. Collander. The permeability of *Nitella* cells to non-electrolytes. *Physiologia Plantarum* **7**:420–445 (1954).
10. R. Collander. On lipid solubility. *Acta Physiol. Scand.* **13**:363–381 (1947).
11. M. H. Abraham. Scales of solute hydrogen bonding—their construction and application to physicochemical and biochemical processes. *Chem. Soc. Revs.* **22**:73–83 (1993).
12. M. H. Abraham, H. S. Chadha, F. Martins, R. C. Mitchell, M. W. Bradbury, and J. A. Gratton. Hydrogen bonding Part 46: A review of the correlation and prediction of transport properties by an LFER method: physicochemical properties, brain penetration, and skin permeability *Pestic. Sci.* **55**:78–88 (1999).
13. M. H. Abraham and J. C. McGowan. The use of characteristic volumes to measure cavity terms in reversed phase liquid chromatography. *Chromatographia* **23**:243–246 (1987).
14. J. A. Platts, D. Butina, M. H. Abraham, and A. Hersey. Estimation of molecular linear free energy relationship descriptors using a group contribution method. *J. Chem. Inf. Comput. Sci.* **39**:835–845 (1999).
15. J. A. Platts, M. H. Abraham, D. Butina, and A. Hersey. *J. Chem. Inf. Comput. Sci.* **40**:71–80 (2000).
16. P. Seiler. Interconversion of lipophilicities from hydrocarbon/water systems into the octanol/water system. *Eur. J. Med. Chem.* **9**:473–479 (1974).
17. N. El Tayar, R. S. Tsai, B. Testa, P.-A. Carrupt, A. J. Leo. Partitioning of solutes in different solvent systems: The contribution of hydrogen-bonding capacity and polarity. *Pharm. Sci.* **80**:590–598 (1991).
18. M. H. Abraham, H. S. Chadha, G. S. Whiting, and R. C. Mitchell. Hydrogen bonding. 32. an analysis of water-octanol and water-alkane partitioning, and the $\Delta\log P$ parameter of Seiler. *J. Pharm. Sci.* **83**:1085–1100 (1994).
19. D. A. Paterson, R. A. Conradi, A. R. Hilgers, T. J. Vidmar, and P. S. Burton. A non-aqueous partitioning system for predicting the oral absorption potential of peptides. *Quant. Struct.-Act. Relat.* **13**:4–10 (1994).
20. M. H. Abraham, F. Martins, R. C. Mitchell, and C. J. Salter. Hydrogen bonding. 47. Characterization of the ethylene glycol-heptane partition system: Hydrogen bond acidity and basicity of peptides. *J. Pharm. Sci.* **88**:241–247 (1999).
21. Y. Ishihama and N. Asakawa. Characterization of lipophilicity scales using vectors from solvation energy descriptors. *J. Pharm. Sci.* **88**: 1305–1312 (1999).